Research Article

Effect of Al$_2$O$_3$ on Optical Absorption Properties of Heavy Metal Oxide Glass System doped with Nd^{3+} Ion

Y.N.Ch.Ravibabu[Å] and S.V.G.V.A.Prasad[B] *

[Å]Department of Physics, The Hindu College, Machilipatnam-521001, A.P, India
[B]Department of Physics, Ideal College of Arts and Sciences (A), Kakinada-533003, A.P, India

Abstract

In this study, the principal role of Al2O3 on the physical properties and the features of the absorption spectra of Nd^{3+} ion doped 20PbO–20Bi$_2$O$_3$-(25-x)MgHPO$_4$-24(25-x) B$_2$O$_3$–1Nd$_2$O$_3$-xAl$_2$O$_3$ (x=1, 2, 3 and 4 mol %) glass system has been investigated. The concentration of Al$_2$O$_3$ is varied from 1 to 4 mol% while that of Nd^{3+} is fixed. Oscillator strengths of hyper sensitive transitions have indicated that there is a gradual decrease in the asymmetry of the glass network with increase in the concentration of Al$_2$O$_3$ up to 4.0 mol%. The Judd–Ofelt theory was successfully applied to characterize Nd^{3+} spectra of all the three glasses. Based on the magnitude of the spectroscopic quality factor Ω$_4$/Ω$_6$, it appears that LBMBPNA1-4 glasses to be a kind of better optical glasses. From this theory various radiative properties, like transition probability A, branching ratio br and the radiative lifetime τ$_R$, for ^{2}H11/2, ^{4}F3/2, ^{4}F9/2 and ^{4}F5/2 levels in the spectra of these glasses have been evaluated. The values of life times for these levels show decreasing order as we increased the Al$_2$O$_3$ content. The reasons for such higher values have been discussed based on the relationship between the structural modifications taking place around the Nd^{3+} ions.

Keywords: *Spectroscopic quality factor, radiative life time, J-O parameters, Polarizability, Al2O3 content, Polaron radius.*

1. Introduction

The Nd^{3+} ions exhibit superior spectroscopic properties in bismuthate glasses advantageous for compact laser applications (Atul *et al*, 2013). Neodymium has been most widely studied as doping agent for use in varieties of applications in the areas like photonic device fabrication, medical diagnostics, communications and optical storage materials (Maciel *et al*, 2006),(Brenier *et al,* 2005),(Sun *et al*, 2006),(Ding *et al*, 2000). Nd^{3+} ion doped glass systems are more prominent among their counter parts for lasing material due to their capabilities to operate with high efficiency even at room temperatures also. The potential ^{4}F$_{3/2}$ → ^{4}I$_{11/2}$ transition of Nd^{3+} ion has more application for high power lasers (Ning Lei *et al*, 1996), (Rao *et al*, 2000),(Hamit Kalayacioglu *et al*, 2008),(Surendra Babu *et al*, 2010).

Structural studies of borophosphate glasses (Yun *et al*,1978),(Ray *et al*,1975), (Brow *et al* ,1990),(Koudelka *et al*, 2000), (Brow *et al*,1997) confirm that boron atoms are incorporated as either trigonal B (3), or tetrahedral B (4), sites within the borophosphate network, depending on composition. In the phosphate-rich range of the composition, boron atoms are mostly B (4), while in the borate-rich range, B (3) dominates. This difference in the coordination number will affect the properties of the glasses. Lead containing glasses are optically transparent from the visible to the near-infrared range, forming a wide compositional regions of PbO content in the host glass matrix considered for incorporation of trivalent rare earth ions (Pisarski *et al*, 2005).

Glasses containing heavy metal oxides, e.g. Bi$_2$O$_3$ and PbO have wide spread applications in the field of glass ceramics, layers for optical and electronic devices, thermal and mechanical sensors, reflecting windows, etc. (Hall *et al*, 1989), (Sugi Moto *et al*, 2002). In glass structure, Pb^{2+} cations play the role of network modifier when these cations are ionically bonded at PbO concentration below 30 mol%. The Pb^{2+} cation will act as glass network former, if Pb–O bond is covalent, conforming the presence of PbO$_3$ and PbO$_4$ structural units at higher PbO content (Sooraj Hussain *et al*, 2006). Bismuth oxide based glasses especially mixed with PbO are well known due to their non-linear optical properties since these glasses posses' high density and high refractive index. Bi$_2$O$_3$ glasses also show far infrared transmission and exhibit luminescence in the NIR region originating from ^{3}P$_1$ level with longer life times (SrinivasaRao *et al*,2011). Bi$_2$O$_3$ based glasses possess high polarizability and exhibit transmission into the far infrared region (in the range 0.5−8.7μm) and show nonlinear optical behavior. In view of such qualities, these glasses find potential applications in optical and optoelectronic devices such as ultrafast switches, infrared windows, optical isolators thermal and mechanical sensors

*Corresponding author: **S.V.G.V.A.Prasad**

(Sidek *et al*, 2005),(Munpakdee *et al*, 2008),(Kityk *et al*, 2002). Although Bi_2O_3 is a weak glass former, because of its highly polarizable nature and density, it participates in the glass network with $[BiO_3]$ pyramidal units and $[BiO_6]$ octahedral units in the presence of glass formers like P_2O_5(Fan et al, 2009).

Al$_2$O$_3$ is a common glass network intermediate. The role of Al$_2$O$_3$ in the glass is dependent on the structure and properties of the glass matrix. Al$_2$O$_3$ which acts like glass network former reacts which the non-bridging oxygen and promotes the formation of bridging oxygen. When there are not adequate non-bridging oxygen in the glass, Al$_2$O$_3$ cannot form the network. Furthermore the Al^{3+} ion electrical field may affect the structure of the network and even lead to the break of the network (JingJing Tong et al,2012). When the heavy metal oxide borophosphate glasses are mixed with different concentrations of Al$_2$O$_3$, we may expect the structural modifications and local field variations around Ln^{3+} ion due to variations in the coordination number of Al^{3+} ions. These changes may have strong bearing on various luminescence transitions and the energy transfer mechanism of rare earth ions in the glass network.

The present study is mainly devoted to investigate the absorption properties of Nd^{3+} ions inBi$_2$O$_3$-PbO-B$_2$O$_3$-MgHPO$_4$ glass system with the relative variations in the concentrations of Al$_2$O$_3$ and MgHPO$_4$ at fixed concentrations of the rare earth ion. Bi$_2$O$_3$ is added to this glass matrix since it favors to widen the glass forming region and further acts as a moisture resistant. The optical band gaps also been studied to have an idea concerning the structural changes in the glass network due to the variations in the concentrations of Al$_2$O$_3$ at the neighborhood of rare earth ions. The Judd-Ofelt analysis has been performed for all the studied Al$_2$O$_3$ concentrations, from which the radiative properties of active ions have been estimated.

2. Experimental

Glasses with chemical compositions in mol% 20 PbO–20Bi$_2$O$_3$-(25-x)MgHPO$_4$-24(25-x) B$_2$O$_3$–1Nd$_2$O$_3$-xAl$_2$O$_3$ (x=1, 2, 3 and 4) were prepared by melt-quenching technique. High purity reagent grade chemicals of H$_3$BO$_3$, Bi$_2$O$_3$, MgHPO$_4$, 3H$_2$O, Al$_2$O$_3$ and Nd$_2$O$_3$ were used as starting materials. The chemical batches were prepared to yield 10 g of glass. Each precisely weighed and mixed chemical batch was taken in a pure porcelain crucible, which then introduced to the melting furnace. The melting was carried out at 1050 ^{0}C temperatures for 45 min and stirred well to ensure melt homogeneity. The cast glasses were annealed at 350 ^{0}C for 1 h and later cooled slowly to the room temperature. The obtained glasses were then cut and polished for various characterizations. All the glasses have been labeled as LBMBPNA1- LBMBPNA4 based on the presence of Al$_2$O$_3$ contents in host glass. The glass density was measured by Archimedes' buoyancy principle using water as immersion liquid on Mettler-Tollado digital balance fitted with a density measurement kit. These density values were used for the estimation of dopant concentration in different glasses needed for various

calculations. The optical absorption spectra were recorded on a UV-Vis-NIR spectrophotometer (Shimadzu, Japan, Model: 3101) in the 300-2750 nm wavelength range.

3. Results and discussion

3.1. Physical properties

Physical properties such as Neodymium ion concentration (N), inter ionic distance (r$_i$), polaron radius (r$_p$), field strength (F), molar refractivity (R$_M$), electronic polarizability (α) and dietric constant are evaluated using relevant expressions (Duffy *et al*, 1975),(Pauling ,1960) ,(Sooraj Hussain *et al*, 2009)for Nd^{3+} doped LBMBPNA1, LBMBPNA2, LBMBPNA3and LBMBPNA4 glasses and is presented in Table 1. The number of luminescent centers is found to be densely distributed because of the fact that the glass density (d) and refractive index (n) values are higher. The polaron radius (r$_p$) is smaller than inter ionic distance (r$_i$) and hence such a smaller r$_p$ value has resulted in a higher field strength (F) shown in Table.1. Polaron radius and inter ionic distances increases with Al$_2$O$_3$ content. The polaron radius, inter ionic distance, electronic polarizability and molar refractivity are observed to be increased with the alluminium content. But the field strength decreases with the increment of Al$_2$O$_3$ content.

3.2. Optical band gap

The absorption spectra of LBMBPNA glasses in the spectral range from 400 to 900 nm are shown in Fig. 1. The observed absorption bands in the visible and NIR regions are attributed to the 4f–4f transitions of Nd^{3+} from the ^{4}I$_{9/2}$ ground state to various excited states.

To understand optically induced transitions and optical band gaps of materials, the study of optical absorption edge gives more important information. The principle of the technique is that a photon with energy greater than the band gap energy will be absorbed. There are two kinds of optical transitions at the fundamental absorption edge: direct and indirect transitions, both of which involve the interaction of an electromagnetic wave with an electron in the valence band.

The optical absorption at the fundamental edge in terms of the theory given by Davis and Mott in general form is as follows.
Equation (1)

where B is a constant, hυ is the optical energy and E$_{opt}$ is the optical band gap. The values of n are ½ and 2 for indirect and direct transitions, respectively (Dow *et al*, 1972),(Carnall   *et al*,1968),(Sontakke *et al*, 2011).The optical band gaps (E$_{opt}$) for both indirect and direct transitions of 20PbO–20Bi$_2$O$_3$-(25-x) MgHPO$_4$-24(25-x) B$_2$O$_3$–1Nd$_2$O$_3$-xAl$_2$O$_3$ (x=1, 2, 3 and 4) glasses are given in Fig.2(a) and Fig.2(b). From this, the optical band gaps (E$_{opt}$) for indirect and direct transitions are found to be increased with the increased Al$_2$O$_3$ content. Al$_2$O$_3$ which acts like glass network former reacts which the non-bridging oxygen and promotes the formation of bridging oxygen. Since NBOs are less excited than bridging

oxygens (BOs), the band gap increased with the increment of Al_2O_3 content as shown in Table 2.

3.3. Absorption spectrum

The observed energy levels of LBMBPN1-4 glasses at about 513 nm, 525 nm, 583 nm, 627 nm, 683 nm, 747 nm, 803 nm and 875 nm were assigned to $^4I_{9/2} \rightarrow ^4G_{9/2}$, $^4G_{7/2}+^2K_{13/2}$, $^4G_{5/2}+^2G_{7/2}$, $^2H_{11/2}$, $^4F_{9/2}$, $^4F_{7/2}+^4S_{3/2}$, $^4F_{5/2}+^2H_{9/2}$ and $^4F_{3/2}$ transitions (Dieke ,1968) respectively. The energy levels lying below 450 nm could not be observed in the present glass system due to intrinsic inter band absorption of the host matrices.

3.3.1. Spectral Intensities

The experimental oscillator strengths (f_{exp}) of all the absorption bands have been measured using the area method in Equation (2)

The f_{cal} values for all those bands are evaluated using Judd-Ofelt theory (Judd ,1962),(Ofelt ,1962) from the given formula. Where ε is the molar extinction coefficient at energy υ cm^{-1}. $\int \varepsilon(\upsilon)\, d\upsilon$ was evaluated using area method. The intensities of all spectral lines (f_{calc}) are evaluated as Equation(3)

'υ' is the mean energy of the transition and $||U^\lambda||^2$ represent the square of the reduced matrix elements of the unit tensor operator $||U^\lambda||^2$ connecting the initial and final states. The $||U^\lambda||^2$ values employed in the present studies obtained from the literature (Carnall et al, 1968). The experimental (f_{exp}) and calculated (f_{cal}) spectral intensities of obtained energy levels of Nd^{3+} are shown in Table 3. The rms deviation between f_{exp} and f_{cal} is very low, confirming the validity of Judd-Ofelt theory (Choi *et al*, 2008).

The hypersensitive transition $^4I_{9/2} \rightarrow ^4G_{5/2}+ ^2G_{7/2}$ of Nd^{3+} ions, obeys the selection rules $\Delta J \leq 2$, $\Delta L \leq 2$ and $\Delta S = 0$. The intensity of hypersensitive transition in all the glass hosts of present study is given in Table.3. These transitions are found to be very sensitive to the environment of the rare earth ion. The intensities of the hyper sensitive transitions in all the present glasses for varying Al_2O_3 content of the host matrices and the variation trend is obtained as follows,

LBMBPN1 > LBMBPN2> LBMBPN3 > LBMBPN4.

3.3.2. Judd- Ofelt parameters

Judd–Ofelt analysis (Judd ,1962),(Ofelt ,1962) has been performed on these eight well resolved observed absorption bands of Nd^{3+} to estimate the three phenomenological intensity parameters ($\Omega_{2,4,6}$) through least square fitting of their experimental line strengths. The values of J-O parameters are found to be in the following order for Nd^{3+} ions: $\Omega_4 > \Omega_6 > \Omega_2$ presented in Table.4. The comparison of the data on Ω_λ parameters of Nd^{3+} ions in various other glass matrices (Atul *et al*, 2013),(Mc Dougall *et al*, 1994),(Moorthy *et al*, 2000),(Sunil Bhardwaj *et al*, 2012) indicated the same trend. The

variation of Ω_2 parameter with the concentration of Al_2O_3 shown in Table.4, exhibits decreasing trend up to 4.0 mol% of Al_2O_3; such a decrease indicates declining interaction of rare earth ions with the ions of the host materials due to increasing distortion or structural change in the vicinity of rare earth ions. The Ω_2 intensity parameters is related to the hypersensitive transition $^4I_{9/2} \rightarrow ^4G_{5/2}$, $^2G_{7/2}$ of Nd^{3+} ions, and thus is useful in understanding the asymmetry of crystal field as well as the degree of covalency of Nd-O bonding. The small value of Ω_2 parameter in present glasses is due to the relatively more symmetric crystal field around dopant ions compared to the other hosts (Balda *et al*,2000). In glass structure, Pb^{2+} cations play the role of a network modifier when these cations are ionically bonded at PbO concentrations below 30 mol% (Ravi Babu et al, 2000). Ω_4 and Ω_6 values depend on bulk properties such as viscosity and dielectric of the media and are also affected by the vibronic transitions of the rare earth ions bound to the ligand atoms (Prakash et al, 2000). The rigidity and dielectric indicative Ω_4 and Ω_6 parameters obtained in the present study for LBMBPNA1-4 glass systems show higher in their magnitudes compared to Ω_2 parameter suggesting the favorable spectroscopic quality of the glass hosts under study. The values of Ω_4 and Ω_6 are strongly influenced by the vibrational levels associated with the central Nd^{3+} ions bound to the ligand atoms. The increment of Al_2O_3 concentration makes the average Nd–O distance to increase and this produces a weaker field around the Nd^{3+} ion leading to lower value of Ω_2 for LBMBPNA1-4. The ratio Ω_4/Ω_6 can be used to predict the stimulated emission of the laser active medium. The good optical properties of the samples were also supported by the large Ω_4/Ω_6 ratio (Bo Zhou et al, 2009). Based on the magnitude of the spectroscopic quality factor Ω_4/Ω_6, it appears that LBMBPNA1-4 glasses to be a kind of better optical glasses. The variation of Ω_4 and Ω_6 parameters with the concentration of Al_2O_3 shown in Table.4, exhibits decreasing trend up to 4.0 mol% of Al_2O_3. The spectroscopic quality factor Ω_4/Ω_6 shows the significant value greater than 1.

3.3.3 Radiative properties

Using Judd–Ofelt intensity parameters, Ω_k (k = 2, 4 and 6) obtained from the measured spectral intensities of the absorption bands and using the formulae given in the theory, the total radiative transition probabilities (A_T) and radiative lifetimes (τ_R) of the excited states $^4G_{9/2}$, $^4G_{7/2}$, $^4G_{5/2}$, $^2H_{11/2}$, $^4F_{9/2}$, $^4F_{5/2}$ and $^4F_{3/2}$ of Nd^{3+}ion in LBMBPNA1-4 have been calculated. The calculated radiative lifetimes of all the above-excited states are presented in Table.5. The above parameters can be evaluated from the following expressions (Judd,1962).

The computed values of electric dipole line strength (S_{ed}), radiative transition probabilities (A_{rad}), radiative life times (τ_R), branching ratios (β) and absorption cross-sections (σ_a) for the exited states $^4G_{9/2}$, $^4G_{7/2}$, $^4G_{5/2}$, $^2H_{11/2}$, $^4F_{9/2}$, $^4F_{5/2}$ and $^4F_{3/2}$ of Nd^{3+}ion in LBMBPN1-4 hosts are calculated and presented in Tables.5 and 6. The above parameters can be evaluated from the following expressions (Ravi Babu et al, 2013).

Equations (4,5,6,7,8,9)

It is interesting to note that the following trend in the magnitudes of the lasing levels is observed as follows: $^2H_{11/2} > {^4}F_{3/2} > {^4}F_{9/2} > {^4}F_{5/2}$

The trend of the life times for the transitions is found to be in the order due to increment of the Al_2O_3 content. LBMBPNA4 > LBMBPNA3 > LBMBPNA2 > LBMBPNA1.

4. 1Figures
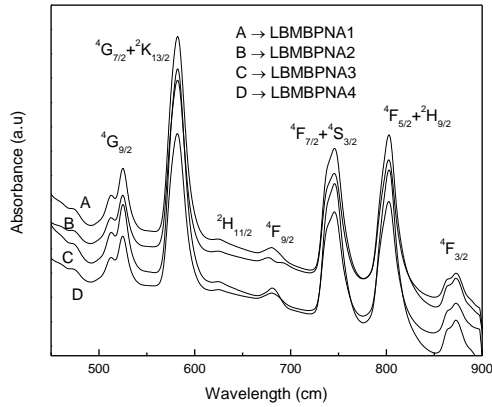
Figure 1 Vis absorption spectra of Nd³⁺ions doped LBMBPNA glasses
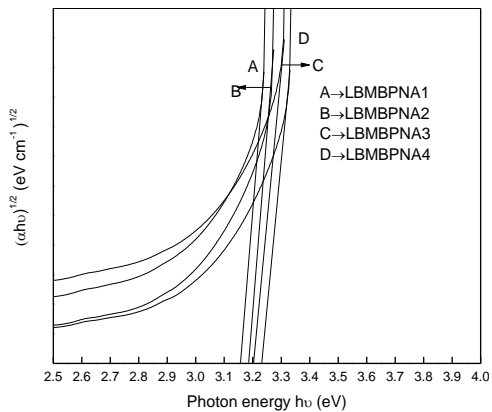
Figure 2 (a). Plot of $(\alpha h\upsilon)^{1/2}$ versus photon energy (hυ) to evaluate indirect band gap energy of LBMBPNA1, LBMBPNA2, LBMBPNA3 and LBMBPNA4 glasses
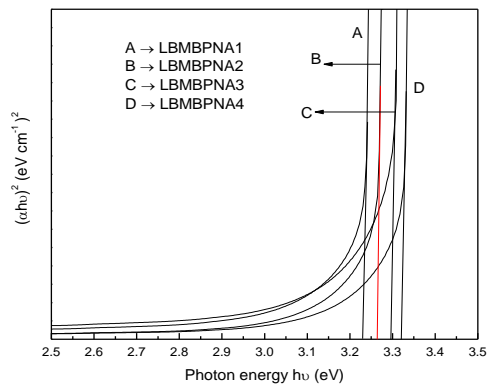
Figure 2 (b) Plot of $(\alpha h\upsilon)^2$ versus photon energy (hυ) to evaluate Direct band gap energy of LBMBPNA1, LBMBPNA2, LBMBPNA3 and LBMBPNA4 glasses.
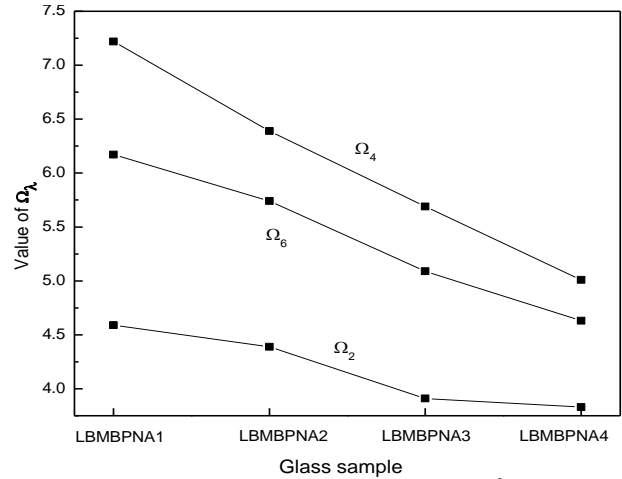
Figure 3 A plot of J-O parameters of Nd³⁺ions doped LBMBPNA1-4 glasses
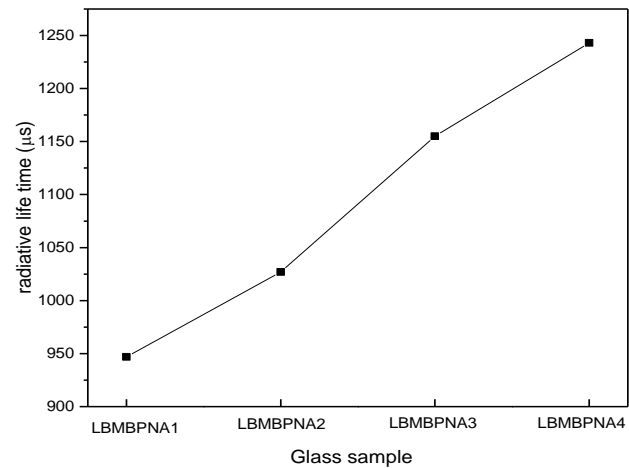
Figure 4 A plot of radiative life times of the transition $^2H_{11/2} \rightarrow {^4}F_{9/2}, {^4}I_{9/2}$ of Nd³⁺ions doped LBMBPNA1-4 glasses.

4.2 Equations

$$\alpha(\nu) = \frac{B}{h\nu(h\nu - E_{opt})^n} \tag{1}$$

$$f_{exp = 4.32 \, X \, 10^{-9} \int \epsilon(\nu)d\nu} \tag{2}$$

$$f_{cal} = \sum_{\lambda=2}^6 T_\lambda \nu(\psi_{J \parallel U^\lambda \parallel}\psi_{J})^2 \tag{3}$$

Electri dipole strength

$$s_{ed = e^2} \sum_{\lambda=2}^6 \Omega_\lambda \, (\psi_J \parallel U^\lambda \parallel \psi' J')^2 \tag{4}$$

Radiative transition probability

$$A_{rad} = \left[\frac{64\,\pi^4\,\nu^3}{3h(2J+1)}\right]\left[\frac{n(n^2+2)}{9}\right]s_{ed} \tag{5}$$

Total radiation probability

$$A_T(\psi_J) = \sum_{\psi_J}^{\psi_J'} A(\psi_J, \psi_{J'}) \tag{6}$$

Radiative life time

$$\tau_R = \frac{1}{A_{T\,(\psi_J)}} \qquad (7)$$

Branching ratio

$$\beta_r(\psi_J, \psi_{J'}) = \frac{A\psi_J, \psi_{J'}}{A_{T\,(\psi_J)}} \qquad (8)$$

$$\sigma_\alpha = \frac{A}{8\pi cn^2\nu^2} \qquad (9)$$

5. Tables

Table 1 Physical properties of Nd3+ ions doped of LBMBPNA1, LBMBPNA2, LBMBPNA3 and LBMBPNA4 glasses

Physical Property	LBMB PNA1	LBMB PNA2	LBMB PNA3	LBMB PNA4
Avg. molecular weight	210.6	209.9	209.2	208.5
Density (ρ) (g/cm3)	4.293	4.253	4.21	4.176
Refractive index 'n'	2.005	2.008	2.011	2.013
Ion concentration N (×1022 ions/cm3)	1.23	1.22	1.21	1.21
Polaron radius rp (Å)	3.75	3.75	3.76	3.77
Inter nuclear distance ri (Å)	4.34	4.34	4.35	4.36
Field Strength F (×1015cm2)	2.14	2.13	2.12	2.11
Molar refraction RM	24.62	24.81	25.02	29.41
Electronic polarizability α (×10-24)	9.76	9.83	9.91	10.09
Molar Volume (VM) (cm3)	49.07	49.36	49.69	49.93
Dielectric constant ε	3.02	3.03	3.04	3.05

Table 2 Computed optical band gaps in (eV) for Nd³⁺ doped LBMBPNA1-4 glasses

Band gap (eV)	LBMB PNA1	LBMB PNA2	LBMB PNA3	LBMB PNA4
Indirect mobility gap	3.15	3.18	3.2	3.23
direct mobility gap	3.22	3.26	3.29	3.32

Table 3 Experimental and calculated spectral intensities (f×10⁻⁶) of LBMBPNA1, LBMBPNA2, LBMBPNA3 and LBMBPNA4 glasses

Transition ⁴I₉/₂→	LBMB PNA1		LBMB PNA2		LBMB PNA3		LBMB PNA4	
	f_exp	f_cal	f_exp	f_cal	f_exp	f_cal	f_exp	f_cal
4F₃/₂	2.62	4.98	2.34	4.45	2.09	3.97	2.34	3.53
⁴F₅/₂	13.1	11.3	11.7	10.3	10.4	9.18	8.83	8.27
⁴F₇/₂	11.8	12.9	11.1	11.9	9.89	10.6	9.33	9.65
⁴F₉/₂	1.04	1.05	0.84	0.97	0.75	0.86	0.26	0.78
²H₁₁/₂	0.19	0.29	0.17	0.27	0.15	0.24	0.15	0.22
⁴G₅/₂	27.2	27.3	25.2	25.4	22.5	22.6	21.2	21.3
⁴G₇/₂	9.75	7.17	9.35	6.49	8.39	5.79	7.39	5.23
⁴G₉/₂	0.58	0.9	0.45	0.82	0.4	0.73	0.45	0.65
rms dev	± 0.12		± 0.12		± 0.12		± 0.1	

Table 4 Judd-Ofelt intensity parameters ($\Omega\lambda \times10^{-20}$) ($\lambda$=2, 4, 6) (cm²) of LBMBPNA1, LBMBPNA2, LBMBPNA3 and LBMBPNA4 glasses

Glass	Ω_2	Ω_4	Ω_6	Ω_4/Ω_6	Order	Reference
LBMB PNA1	4.59	7.22	6.17	1.17	$\Omega_4 > \Omega_6 > \Omega_6$	Present
LBMB PNA2	4.39	6.39	5.74	1.11	$\Omega_4 > \Omega_6 > \Omega_6$	Present
LBMB PNA3	3.91	5.69	5.09	1.12	$\Omega_4 > \Omega_6 > \Omega_6$	Present
LBMB PNA4	3.83	5.01	4.63	1.08	$\Omega_4 > \Omega_6 > \Omega_6$	Present
NO1	2.409	4.294	3.504	1.22	$\Omega_4 > \Omega_6 > \Omega_6$	[1]
NO3	2.414	4.133	3.461	1.19	$\Omega_4 > \Omega_6 > \Omega_6$	[1]
ZBLAN	0.94	6.54	3.84	1.7	$\Omega_4 > \Omega_6 > \Omega_6$	[36]
CLBP	1.53	4.86	2.77	1.75	$\Omega_4 > \Omega_6 > \Omega_6$	[37]
BBSN1	3.52	4.19	3.86	1.08	$\Omega_4 > \Omega_6 > \Omega_6$	[38]
BBSN2	3.22	5.05	4.94	1.02	$\Omega_4 > \Omega_6 > \Omega_6$	[38]

Table 5 Transition probabilities (A) in s⁻¹, Total transition probabilities (AT) in s⁻¹, Radiative lifetimes (τR) in 'μs' and branching ratios (β) for the fluorescent states of Nd³⁺ions doped in LBMBPNA1, LBMBPNA2, LBMBPNA3 and LBMBPNA4 glasses

Transition		LBMB PNA1		LBMB PNA2		LBMB PNA3		LBMB PNA4	
SLJ	S'L'J'	A	β	A	β	A	β	A	β
²H₁₁/₂	⁴F₉/₂	0.782	0	0.733	0	0.653	0	0.623	0
	⁴F₇/₂	9.177	0.008	8.566	0.008	7.597	0.008	7.041	0.008
	⁴S₃/₂	2.891	0.002	2.572	0.002	2.291	0.002	2.037	0.002
	⁴F₅/₂	3.745	0.003	3.478	0.003	3.082	0.003	2.822	0.003
	²H₉/₂	33.85	0.032	31.74	0.032	28.14	0.032	26.17	0.032
	⁴F₃/₂	2.422	0.002	2.262	0.002	2.003	0.002	1.841	0.002
	⁴I₁₅/₂	528.2	0.5	489.8	0.503	436.4	0.503	412.4	0.512
	⁴I₁₃/₂	136.1	0.128	122.9	0.126	109.4	0.126	99.09	0.123
	⁴I₁₁/₂	171.6	0.162	156.8	0.161	139.4	0.161	127.5	0.158
	⁴I₉/₂	167.1	0.158	154.4	0.158	136.9	0.158	124.9	0.155
	A_T	1056		973.4		866		804.6	
	τ_R	947		1027		1155		1243	
⁴F₉/₂	⁴F₇/₂	1.915	0	1.766	0	1.57	0	1.455	0
	⁴S₃/₂	0.017	0	0.016	0	0.014	0	0.012	0
	⁴F₅/₂	7.118	0.001	6.55	0.001	5.813	0.001	5.306	0.001
	²H₉/₂	1.038	0	0.989	0	0.881	0	0.862	0
	⁴F₃/₂	14.87	0.001	13.86	0.001	12.28	0.001	11.27	0.001
	⁴I₁₅/₂	2447	0.256	2224	0.253	1976	0.253	1784	0.251
	⁴I₁₃/₂	3412	0.357	3138	0.357	2784	0.357	2533	0.356
	⁴I₁₁/₂	3063	0.321	2850	0.324	2525	0.324	2315	0.326
	⁴I₉/₂	593.2	0.062	548.9	0.062	486.7	0.062	445	0.062
	A_T	9542		8785		7793		7096	
	τ_R	105		114		128		141	
⁴F₅/₂	²H₉/₂	0.009	0	0.008	0	0.007	0	0.007	0
	⁴F₃/₂	0.816	0	0.753	0	0.671	0	0.63	0
	⁴I₁₅/₂	365	0.03	341.2	0.03	302.1	0.03	277.8	0.031
	⁴I₁₃/₂	2268	0.188	2083	0.188	1848	0.188	1680	0.189
	⁴I₁₁/₂	1650	0.136	1478	0.134	1315	0.134	1176	0.132
	⁴I₉/₂	7776	0.644	7122	0.645	6322	0.645	5736	0.646
	A_T	12061		11027		9789		8872	
	τ_R	82.5		90.7		102		113	
⁴F₃/₂	⁴I₁₅/₂	39.16	0.004	36.59	0.004	32.4	0.004	29.8	0.004
	⁴I₁₃/₂	783.9	0.082	732.6	0.084	648.7	0.083	596.6	0.085
	⁴I₁₁/₂	4418	0.462	4070	0.468	3610	0.467	3289	0.47
	⁴I₉/₂	4303	0.45	3858	0.443	3433	0.444	3070	0.439
	A_T	9545		8698		7725		6985	
	τ_R	105		115		129		143	

Table.6. Electric dipole line strengths (Sed/e² × 10²²) in cm⁻² and Integrated absorption cross sections ($\sigma_a \times 10^{-18}$)(cm⁻¹) of Nd³⁺ ions doped in LBMBPNA1, LBMBPNA2, LBMBPNA3 and LBMBPNA4 Glasses

Transition		LBMB PNA1		LBMB PNA2		LBMB PNA3		LBMB PNA4	
SLJ	S'L'J'	S_{ed}	σ_a	S_{ed}	σ_a	S_{ed}	σ_a	S_{ed}	σ_a
$^2H_{11/2}$	$^4F_{9/2}$	67.96	0.135	63.44	0.126	56.47	0.112	53.37	0.107
	$^4F_{7/2}$	105.9	0.412	98.48	0.385	87.34	0.341	80.21	0.316
	$^4S_{3/2}$	41.63	0.150	36.87	0.134	32.83	0.119	28.94	0.106
	$^4F_{5/2}$	16.91	0.090	15.64	0.083	13.85	0.074	12.57	0.067
	$^2H_{9/2}$	204.2	0.988	190.7	0.926	169.0	0.821	155.8	0.764
	$^4F_{3/2}$	5.071	0.034	4.715	0.032	4.175	0.028	3.803	0.026
	$^4I_{15/2}$	108.9	1.624	100.5	1.506	89.63	1.341	83.93	1.268
	$^4I_{13/2}$	15.89	0.286	14.27	0.258	12.71	0.230	11.40	0.208
	$^4I_{11/2}$	12.58	0.264	11.44	0.241	10.18	0.215	9.228	0.196
	$^4I_{9/2}$	8.368	0.199	7.696	0.184	6.824	0.163	6.171	0.149
$^4F_{9/2}$	$^4F_{7/2}$	157.0	0.359	144.1	0.331	128.2	0.294	117.7	0.273
	$^4S_{3/2}$	2.339	0.004	2.100	0.004	1.867	0.003	1.661	0.003
	$^4F_{5/2}$	108.8	0.436	99.69	0.401	88.48	0.356	80.01	0.325
	$^2H_{9/2}$	25.57	0.087	24.25	0.083	21.60	0.074	20.93	0.072
	$^4F_{3/2}$	72.14	0.423	66.96	0.395	59.31	0.350	53.96	0.321
	$^4I_{15/2}$	646.6	10.02	585.0	9.108	519.7	8.091	464.9	7.304
	$^4I_{13/2}$	471.3	9.067	431.4	8.337	382.7	7.397	345.1	6.730
	$^4I_{11/2}$	252.2	5.765	233.5	5.363	206.9	4.751	187.9	4.356
	$^4I_{9/2}$	32.11	0.844	29.58	0.781	26.23	0.692	23.76	0.633
$^4F_{5/2}$	$^2H_{9/2}$	28.29	0.027	25.37	0.024	22.58	0.022	20.21	0.020
	$^4F_{3/2}$	73.98	0.230	67.95	0.212	60.54	0.189	56.30	0.17768
	$^4I_{15/2}$	141.9	2.718	132.0	2.540	116.9	2.250	106.5	2.069
	$^4I_{13/2}$	378.6	9.613	346.3	8.831	307.2	7.835	276.8	7.124
	$^4I_{11/2}$	145.3	4.567	129.6	4.091	115.3	3.640	102.1	3.254
	$^4I_{9/2}$	414.8	15.40	378.2	14.10	335.7	12.52	301.8	11.36
$^4F_{3/2}$	$^4I_{15/2}$	17.28	0.415	16.07	0.388	14.23	0.344	12.97	0.316
	$^4I_{13/2}$	129.1	4.316	120.1	4.033	106.4	3.572	96.97	3.284
	$^4I_{11/2}$	354.7	15.06	325.3	13.87	288.5	12.30	260.4	11.21
	$^4I_{9/2}$	199.0	10.15	177.5	9.104	158.0	8.101	140.0	7.245

Conclusion

The spectroscopic properties of Nd³⁺ ions doped glasses have been analyzed on the basis of Judd-Ofelt theory. The intensity parameter Ω_2 is most sensitive to the local environment of Nd³⁺ ions, larger values ($\Omega_2 > 3.5$) suggest a less Centro symmetric coordination environment. The spectroscopic quality factor Ω_4/Ω_6 is enhanced due to the addition of Al₂O₃ to LBMBPN glasses. The branching ratio for the $^4F_{3/2} \rightarrow {}^4I_{11/2}$ transition in the present glass is 47% and the predicted spontaneous radiative transition rate is as high as 3289 s⁻¹ for LBMBPNA4 sample. The results of these investigations indicate that neodymium doped allumino lead bismuth borophosphate glasses may be suitable host for the lasing materials. The optical absorbance analysis of these glasses confirmed the decrease in both the NBOs and the molar volume, which in turn explain the obtained decrease in the covalency, an increase in the optical band gap of the studied glasses.

References

D. Atul ,Sontakke, K. Annapurna, (2013), Spectroscopic properties and concentration effects on luminescence behavior of Nd³⁺ doped Zinc–Boro–Bismuthate glasses *Materials Chemistry and Physics*, 137, pp 916-921.

G. S. Maciel, N.Rakov, M.Fokine,C.S. CarvlhoI ,(2006), Strong upconversion from Er₃Al₅O₁₂ ceramic powders prepared by low temperature direct combustion synthesis *Appl. Phys. Lett* ,89, pp 0811091-0811093.

A. Brenier, C.Tu, Z.Zhu, J.Li, B.Wu, (2005), Yellow and infrared self-frequency conversions in GdAl₃ (BO₃) (4): Nd³⁺*J. Appl. Phys*, 97, 013503.

H. Sun, L. Zhang, M.Liao, G. Zhou, C.Tu, J.Zhang, L.Hu, S. Jiang ,(2006) , Host dependent frequency upconversion of Er³⁺-doped oxyfluoride germanate glasses , J. Lumin, 117 , pp 179-186.

Y. Ding, S. Jiang, R. C. Hwang, T. Luo, T. Peyghambarian, Y.Himei, T. Ito, T. Miura,(2000), Spectral properties of erbium-doped lead halotellurite glasses for 1.5 mu m broadband amplification *Opt. Mater*, 15, pp 123-130.

T. V. R Rao, R. R Reddy, Y. Nazeer Ahmmed, M.Parandharmaiah, N.Sooraj Hussain, *S. Buddhudu, K. Purandhar,*(2000)*, Luminescence properties of Nd³⁺: TeO₂–B₂O₃–P₂O₅–Li₂O glass, Infrared phys. Technol* , 41 ,247.

Hamit Kalayacioglu, Huseyin Cankaya, Gonul ozen, Lutfu ovecoglu, Alphan Sennaroglu,(2008), Lasing at 1065 nm in bulk Nd3+-doped telluride-tungstate glass,*Opt. Commun* , 281, pp 6056-6060.

S. Surendra Babu, R. Rajeswari, WanJang, Cho Eun Jin, Kyoung Hynk Jang, HyoJin Sco, C.K. Jaya Sankar,(2010), Spectroscopic investigations of 1.06 μm emission in Nd3+-doped alkali niobium zinc tellurite glasses ,*J.Lumin* ,130, pp 1021-1025.

H. Yun, P.J. Bray, (1978), Nuclear magnetic resonance studies of the glasse in the system,K_2O-B_2O_3-P_2O_5, *J. Non- Cryst. Solids,* 30, pp 45-60.

N.H. Ray, (1975), A Study of the Coordination of Boron in Potassium Borophosphate Glasses by Raman Spectroscopy , *Phys. Chem. Glasses*, 16 , pp 75-80.

R. K. Brow, (1996), An XPS Study of Oxygen Bonding in Zinc Phosphate and Zinc Borophosphate Glasses, *J.Non-Cryst. Solids*, 194, pp 267-273.

L.Koudelka,P.Mosner,(2000),Borophosphate glasses of The ZnO-B_2O_3-P_2O_5 system, gla glasses *Mater. Lett* 42, pp 194-199.

R.K. Brow, D.R. Tallant, (1997) Structural Design of Sealing Glasses,*J. Non-Cryst. Solids*, 222, pp 396-406.

W.A. Pisarski, T. Goryczka, B. Wodecka-Dus, M. Paonska, J. Pisarska, (2005) , Structure and properties of rare earth - doped lead borate glasses, *Materials Science and Engineering B* ,122, pp 94-99.

D.W. Hall, M.A. Newhouse, N.F. Borrelli, W.H. Dumbaugh, D.L.Weidman, (1989),Nonlinear optical susceptibilities of high-index glasses, *Appl. Phys.Lett,* 54, pp 1293-1295.

N. Sugi Moto, (2002) , Ultrafast Optical Switches and Wavelength Division Multiplexing (WDM) Amplifiers Based on Bismuth Oxide Glasses ,*J. Am. Ceram. Soc.*, 85, pp 1083-1088.

N. Sooraj Hussain, N. Ali, A.G. Dias, M.A. Lopes, J.D. Santos, S. Buddhudu , (2006) ,Absorption and emission properties of Ho^{3+} doped lead–zinc–borate glasses, *Thin Solid Films ,*515, pp 318 – 325.

N. SrinivasaRao, P.RaghavaRao, Y.Gandhi, Ch.SrinivasaRao, G.SahayaBaskaran, V. RaviKumar, N.Veeraiah, (2011) , Investigation on spectral features of tungsten ions in PbO–Bi_2O_3–As_2O_3 glass matrix, *Physica B*, 406, pp 4494–4499.

H.A.A. Sidek, M. Hamezan, A.W. Zaidan, Z.A. Talib, K. Kaida, (2005) ,Optical Characterization of Lead-Bismuth Phosphate Glasses,*Am. J. Appl. Sci.*, 2 , pp 1266-1269.

A. Munpakdee, K. Pengpat, T. Tunkasiri, D. Holland, (2008), Ferroelectric glass ceramics from the PbO-Bi_2O_3 –GeO_2 system, *Adv. Mater. Res,.* 55, pp 473-476.

V. Kityk, J. Wasylak, J. Kucharski, D. Dorosz, (2002), PbO–Bi_2O_3–Ga_2O_3–BaO–Dy^{3+} glasses for IR luminescence, J. Non-Cryst. Solids, 297, pp 285-289.

H. Fan, G. Wang, L. Hu, Infrared, (2009)**,** Raman and XPS spectroscopic studies of Bi_2O_3–B_2O_3–Ga_2O_3glasses**,** *Solid State Sci.*, 11**,** pp 2065**-**2070.

JingJing Tong, MinFang Han , Subhash C. Singhal, Yudong Gong, Influence of Al_2O_3 addition on the properties of Bi_2O_3–BaO–SiO_2–R_xO_y (R=K, Zn, etc.) glass sealant, (2012), *Journal of Non-Crystalline Solids*, 358, pp 1038–1043.

A. Duffy, M .D. Ingram, (1975), An interpretation of glass chemistry in terms of the optical basicity concept, *J. Inorg. Nucl. Chem.*, 37, pp 1203-1203.

L. Pauling ,1960, *The Nature of Chemical Bond 3rd edn* (Ithaca, NY: Cornell University Press) 93.

N. Sooraj Hussain, P .J. Cardoso, G. Hungerford, M .J.M Gomes, Nasar Ali, J. D. Santos,S. Buddhdu, (2009), Physical and optical characterization of Er3+ doped Lead-zinc-borate glass,*J. Nanosci. Nanotechnol* , 9, pp 3555-3561.

D. Dow, D. Red Field , (1972), Toward a unified theory of Urbach's rule and exponential absorption edges, *Phys. Rev.*, B5, 594.

W.T. Carnall, P.R. Fields, K. Rajnak , (1968) ,Spectral Intensities of the Trivalent Lanthanides and Actinides in Solution. II. Pm^{3+}, Sm^{3+}, Eu^{3+}, Gd^{3+}, Tb^{3+}, Dy^{3+}, and Ho^{3+} , *J. Chem. Phys.*, 49, pp 4412-4423

A.D. Sontakke, K. Biswas, A. Tarafder, R. Sen, K. Annapurna , (2011) ,Broadband Er^{3+} emission in highly nonlinear bismuth modified zinc–borate glasses, *Opt Mater. Exp.,* 1, pp 344–356.

G. H. Dieke; Spectra and energy levels of Rare Earth ions in Crystals, *Inter science Publishers New York* (1968).

B R Judd, (1962), Optical Absorption Intensities of Rare-Earth Ions, *Phys. Rev*, pp 127, 750.

G S Ofelt,(1962) , Intensities of Crystal Spectra of Rare Earth Ions, *J Chem Phys*, 37, 511.

Ju H Choi, Frank G Shi, Alfred Margaryan, Ashot Margaryan, Wytze van derVeer, (2008) , Novel Alkaline-Free Er ³ Doped Fluorophosphate Glasses for Broadband Optical Fiber Lasers and Amplifiers, *Alloys and Comp*, 450, pp 540-545.

R. Balda, J. Fernández, M. Sanz, A. de Pablos, J.M. Fdez-Navarro, J. Mugnier, (2000) , Laser spectroscopy of Nd^{3+} ions in GeO_2-PbO-Bi_2O_3 glasses,*Phys. Rev.,* B 61, pp 3384-3390.

Mc Dougall J, Hollis D B & Payne M J B, (1994) Judd-of elt parameters of rare-earth ions in zblali, zblan and zblak fluoride glass, *Phys Chem Glasses*, 35, pp 258-259.

L .R .Moorthy, T. S. Rao, K. Janardhanam, A. Radhaoathy, (2000), Optical absorption and emission properties of Pr(III) in alkali chloroborophosphate glasses , *J. Alloys. Compd* ,298, pp 59-67.

Sunil Bhardwaj, Rajni Shukla, Sujata Sanghi, Ashish Agarwal, Inder Pal, (2012), Optical Absorption and Fluorescence Spectral Analysis of Nd^{3+}Doped Bismuth Boro-Silicate Glasses , *Inter. J.Modern Engg. Res.,* 2, pp 3829-3834.

Y.N. Ch. Ravi Babu, P. Sree Ramnaik, A. Suresh Kumar, (2013), Photoluminescence features of Ho^{3+} ion doped PbO–Bi_2O_3 borophosphate glass systems, *J.Lumin.*, 143*,* pp 510–516.

G.V. Prakash, (2000), Absorption spectral studies of rare earth ions (Pr^{3+}, Nd^{3+}, Sm^{3+}, $Dy^{3+,}$ Ho^{3+} and Er^{3+}) doped in NASICON type phosphate glass, $Na_4AlZnP_3O_{12}$,Mater. Lett. ,46 , pp 15-20.

Bo Zhou, Edwin Yue-Bun Pun, Hai Lin, Dianlai Yang, Lihui Huang, (2009) ,Judd–Ofelt analysis, frequency upconversion, and infrared photoluminescence of Ho^{3+} doped and Ho3$^+$/Yb^{3+}-codoped lead bismuth gallate oxide glasses ,*J. Appl. Phys.,*106 ,103105.

Y. C Ratnakaram, A. ViswanadhaReddy, R.P.S. Chakradhar, (2002) , Electronic absorption spectra and energy gap studies of Er3+ ions in different chlorophosphate glasses, *Spectrochim. Acta A*, 58, pp 1809-1822.